Solvation of Sodium Dimer in Ammonia Clusters: Photoelectron Spectroscopy and ab Initio Study of $Na_2^-(NH_3)_n$

Ryozo Takasu, Kenro Hashimoto,*,† Rei Okuda,† and Kiyokazu Fuke*

Department of Chemistry, Kobe University, Nada, Kobe 657-8501, Japan, and Computer Center, Tokyo Metropolitan University, 1-1 Minami-Ohsawa, Hachioji-shi, Tokyo 192-0397, Japan

Received: August 6, 1998; In Final Form: November 9, 1998

Photoelectron spectra (PESs) of $Na_2^-(NH_3)_n$ ($n = 0-5$) are investigated to explore the solvation of sodium dimer in small ammonia clusters. We also calculate the structures and energetics of $Na_2^-(NH_3)_n$ ($n = 0-3$) as well as the vertical detachment energies (VDEs) associated with the transitions to various neutral states for n up to 2 by using an ab initio MO method. The PES of $Na_2^-(NH_3)$ exhibits five bands at the VDE of 0.41, 1.36, 1.86, 2.11, and 2.40 eV. These bands are reproduced theoretically with a reasonable accuracy and assigned to the transitions from the anion ground state, $1^2\Sigma_u^+(X^-)$, to the neutral ground, $1^1\Sigma_g^+(X)$, and low-lying four excited states derived from the $1^3\Sigma_u^+(a)$, $1^3\Pi_u(b)$, $1^1\Sigma_u^+(A)$, and $1^3\Sigma_g^+$ states of Na_2, respectively. The VDEs to the neutral ground state for all clusters examined are found to be slightly smaller than or equal to that of $Na_2(1^1\Sigma_g^+)$, while that to the first excited state derived from $Na_2(1^3\Sigma_u^+)$ increases gradually for $n = 4$ and 5. In addition, the higher-energy transitions derived from the $1^3\Pi_u$, $1^1\Sigma_u^+$, and $1^3\Sigma_g^+$ states correlated to the $Na(3^2S) + Na(3^2P)$ asymptote are found to be shifted rapidly to the red and almost become degenerate with the $1^3\Sigma_u^+$-type transition. On the basis of these experimental and theoretical results, we discuss the structure of the anion clusters and the solvation state of Na_2 in $(NH_3)_n$.

1. Introduction

Solvated electrons have been studied for more than a century since the first observation by Weyl in 1886. Recent advances in ultrafast laser spectroscopy have renewed efforts to unveil the solvation dynamics of electrons in polar solvent. Despite many efforts, the structure and localization mode of solvated electrons are still the subject of intensive discussion.[1−3] Recently, a new approach such as the study of solvated electrons in finite clusters was started to reveal the microscopic aspect of the solvation state of electrons. Negatively charged water and ammonia clusters, $(H_2O)_n^-$ and $(NH_3)_n^-$, were prepared via capture of low-energy electrons by solvent clusters.[4,5] Photoelectron spectroscopy was conducted for these clusters: n up to ~70 for $(H_2O)_n^-$ and 1100 for $(NH_3)_n^-$.[6,7] The excess electron states were examined using quantum path integral molecular dynamics simulations.[8,9] In order to characterize the localization modes of electron, absorption spectroscopy were also conducted for $(H_2O)_n^-$.[10]

The other interesting target is the clusters consisting of a single alkali atom and solvent molecules. These systems may allow us to construct a model for the well-known bulk solvated electrons in dilute alkali metal solutions at the molecular level. With a view to probe an ion-pair state in clusters, which is a counterpart of bulk solvated electrons, Hertel's and our groups have examined the photoionization processes of solvated alkali-metal atoms as a function of cluster size.[11−14] These studies have shown that the ionization potentials (IPs) of $M(NH_3)_n$ (M = Li,[13] Na,[11] and Cs[12]) with $n \geq 4$ are metal-independent and decrease almost linearly with $(n + 1)^{-1/3}$. For $M(H_2O)_n$ (M = Li,[14] Na,[11] and Cs[12]), IPs for $n \geq 4$ have found to exhibit an anomalous feature; those are metal-independent and become constant at 3.1 ± 0.1 eV. In order to explain the cluster size dependence of IPs and to examine the solvation state of metal atoms in clusters, extensive theoretical calculations have been carried out by several groups.[15−21]

Recently, we have also investigated the electronic structures of $Li(NH_3)_n$, $Na(NH_3)_n$, $Na(H_2O)_n$, and $Li(H_2O)_n$ both in the neutral ground and higher excited states with photoelectron spectroscopy of their anions and ab initio calculations.[13,14,22,23] In order to facilitate comparison between the present results on $Na_2^-(NH_3)_n$ described in the latter section with those of single metal atom, we briefly summarize the results on the alkali atom−ammonia systems. For $M^-(NH_3)$ (M = Li and Na), we have found two isomers such as those with M−N and M−H bonds: The former is calculated to be more stable than the latter by ~1 kcal/mol with zero-point vibrational energy correction. For $n \geq 2$, the isomer with the maximum numbers of M−N bonds has been found to become increasingly stable as n grows and has been observed predominantly in the photoelectron spectra (PESs). In the PESs of $M^-(NH_3)_n$, the vertical detachment energy (VDE) to the neutral ground (^{2}S-type) states is found to be shifted slightly to the lower electron binding energy (EBE) with respect to that of the bare metal anions: The results clearly indicate the larger solvation energy of the neutral clusters than that of the cluster anions. As for $Na^-(NH_3)_n$, the 3^2P-type transition is shifted rapidly to the lower EBE for $n = 4$ and is shifted further with much slower rate for $n \geq 5$. Quite recently, Hertel and Schulz[24] have examined the absorption spectra of $Na(NH_3)_n$ and found the similar drastic change in the excitation energy for the 3p−3s transition of the Na atom. In our previous papers,[14,22] the rapid change in the rate of shift between $n = 4$ and 5 has been ascribed to the formation of solvation shell about Na^-. The 2^2P-type transition of $Li^-(NH_3)_n$ has also found to be shifted to the lower EBE as large as 1.4 eV and almost becomes degenerate with the transition to the neutral ground

* To whom correspondence should be addressed.
† Tokyo Metropolitan University.

10.1021/jp9832948 CCC: $18.00
Published on Web 12/31/1998

(^{2}S) state for $n \geq 10$.[13,14] These results have been analyzed by ab initio calculations and explained in terms of the delocalization of the singly occupied molecular orbital (SOMO) originated mainly from the metal s valence orbital.[21] For $n \geq 3$, the SOMO densities of $Li(NH_3)_n$ and $Na(NH_3)_n$ are calculated to extend in space on and between the ammonia molecules rather than on the metal atom because of the strong metal atom−N interaction, and as a result, the clusters form a one-center ion-pair state.[22,32] Therefore, both the experimental and theoretical results indicate that alkali atom is spontaneously ionized in small ammonia clusters and its valence electron is extensively delocalized over the solvent molecules.

In the present work, we extend the above studies to the ammonia clusters containing sodium dimer to explore further on the early stage of solvated-electron formation and to link the macroscopic with microscopic properties of alkali metal−solvent systems. In contrast to the Na atom, Na_2 may have much larger polarizability and thus its interaction with the solvent molecules is expected to change substantially. And also, since the symmetry of solute is lowered from spherical, it is interesting to know whether the solvation structure is symmetrical or not. In order to gain information on these issues, we have carried out the photoelectron spectroscopy of $Na_2^-(NH_3)_n$ ($n \leq 5$). We have also examined the structure and energetics of $Na_2^-(NH_3)_n$ as well as the VDEs to various states in the neutral clusters by ab initio MO method. The spectra are found to exhibit a drastic decrease in VDEs for the transitions to the neutral excited states, except for the first excited state derived from $Na_2(1^3\Sigma_u^+)$. In addition, the photoelectron band of the transition to the neutral ground state is found to be slightly red-shifted by solvation. In cooperation with the ab initio calculations, we discuss these results in relation to the solvation state of Na_2 in ammonia clusters.

2. Experimental Section

Details of the experimental apparatus for photoelectron spectroscopy used in the present work have been described elsewhere[14,25] and only a brief account will be given here. The apparatus consists of three-stage differentially evacuated chambers: a negative ion source, a TOF mass spectrometer, and a magnetic-bottle type photoelectron spectrometer. Negatively charged sodium−ammonia clusters are produced by a laser vaporization method. Neat ammonia gas of ca. 1 atm is pulsed by a pulsed valve (R. M. Jordan Co. PSV) into a conical channel dug in an aluminum block. Second harmonic of a Nd:YAG laser (Continuum, YG-661) is focused onto the sodium rod (5 mm in diameter) which is rotating and translating in the aluminum block. The metal atoms and clusters vaporized are entrained by the stream of ammonia gas in the channel and are expanded into the first differential vacuum chamber. The negative ions produced are accelerated to 800 eV in a Wiley−McLaren type TOF mass spectrometer by pulsed electric fields. For the photoelectron kinetic energy measurement, negative ions with a given mass-to-charge ratio are selected with a pulsed mass gate after flying 0.9 m, and are decelerated to several tens of eV with a pulsed potential switching method. Decelerated ions are irradiated with the third harmonic of a Nd:YAG laser (Quanta-Ray, GCR-12, typical laser fluence of ca. 5 mJ/cm^2). The kinetic energy of the detached electrons is analyzed by the magnetic bottle type photoelectron spectrometer. The optimized strength of magnetic fields at the detachment region and in the electron flight tube are about 800 and 2 G, respectively, and the resolution of the photoelectron spectra is about 90 meV for the 1.23 eV peak of the Cu^- ion with a detachment photon energy of 3.50 eV. The electron signals are accumulated as a function of flight time in a digital storage oscilloscope (LeCroy 7200A).

3. Computational Method

Molecular structures of $Na_2^-(NH_3)_n$ ($n = 0-2$) are at first optimized at the restricted Hartree−Fock level with the 6-31++G(d,p) basis sets, i.e., ROHF/6-31++G(d,p), and vibrational analyses are carried out by using the analytical second derivative matrix to characterize the stationary points on the potential surface. The geometrical parameters of the minimum structures are refined using the complete active space SCF (CASSCF) method with the same basis sets by keeping their molecular symmetries unchanged from those by ROHF method. The active orbitals in the CASSCF correspond to the $4\sigma_g$, $4\sigma_u$, $5\sigma_g$, $2\pi_u$, $2\pi_g$, $5\sigma_u$, $6\sigma_g$, and $6\sigma_u$ of Na_2 and three σ^* orbitals of N−H bonds in NH_3 (CAS(3E/10+3n MO)).

The VDEs are evaluated by the single and double excitation configuration interaction (SDCI) method with the CASSCF reference space.[26−30] The active orbitals in the CASSCF+SDCI procedure for $n = 0-1$ are the same as those in the calculations for the geometry optimization, while five high-energy orbitals corresponding to the $2\pi_g$, $5\sigma_u$, $6\sigma_g$, and $6\sigma_u$ of Na_2 are not included for $n = 2$ due to the program limit for the CI. The natural orbitals obtained in the preceding CASSCF calculations are used in the CI.

To investigate the transitions to the excited states, the SDCI method preceded by the state-average CASSCF is applied. The numbers of active electrons and orbitals in the CASSCF are the same as those in the above ground-state calculations. Seven states corresponding to $1^1\Sigma_g^+$, $1^1\Sigma_u^+$, $2^1\Sigma_g^+$, $1^1\Pi_u$, and $1^1\Pi_g$ of Na_2 are averaged for singlet. On the other hand, the states derived from $1^3\Sigma_u^+$, $1^3\Pi_u$, $1^3\Sigma_g^+$, $2^3\Sigma_u^+$, and $1^3\Pi_g$ in Na_2 are taken into account for triplet. The $1^1\Sigma_g^+$ and $1^3\Sigma_u^+$ states correlate to the Na(3^2S) + Na(3^2S) asymptote and others to the Na(3^2S) + Na(3^2P) asymptote at the dissociation limit. The VDEs to the neutral excited states are estimated as the sum of the VDE to the neutral ground state and the excitation energies of each neutral state.

The programs used are GAMESS[31] for the geometry optimization, and MOLPRO-96[32] for SDCI.

4. Results and Discussion

As reported in the previous paper,[14] the TOF mass spectrum of negative ions of the sodium−ammonia system produced by the laser vaporization method exhibits the cluster ion signals of $Na_2^-(NH_3)_n$ ($n \leq 10$) in addition to the cluster ions containing a single sodium atom. The abundance of these ions varies with the fluence of vaporization laser and also with the delay time between the pulsed-valve and vaporization laser. We carefully adjust these experimental conditions to maximize the abundance of $Na_2^-(NH_3)_n$ in the molecular beam.

Figure 1 shows the photoelectron spectra of $Na_2^-(NH_3)_n$ ($n = 0-5$) recorded at the detachment energy of 3.50 eV. The optimized structures of $Na_2^-(NH_3)_n$ ($n = 0-2$) together with total binding energies are presented in Figure 2. VDEs for the neutral ground and low-lying excited states are listed in Tables 1 and 2. As shown in Figure 1a, Na_2^- exhibits three PES bands at 0.55, 1.38, and 2.32 eV. The spectrum is almost the same as those reported by Bowen and co-workers.[33] Their results have

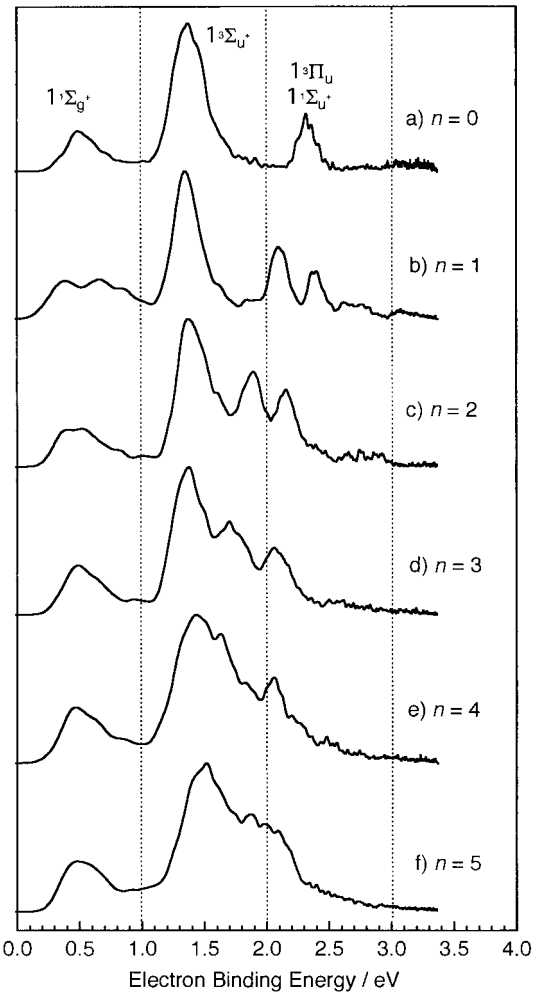

Figure 1. Photoelectron spectra of $Na_2^-(NH_3)_n$ ($n \leq 5$) recorded with the photodetachment wavelength of 355 nm (3.50 eV). The intensities are normalized at the bands corresponding to the $1^3\Sigma_u^+ - 1^2\Sigma_u^+$ transition of Na_2^-.

been analyzed theoretically by Bonacic-Koutecky and co-workers using an ab initio MO method.[34,35] The latter authors have assigned the 0.55 and 1.38 eV bands to the transitions from the ground-state anion, $1^2\Sigma_u^+(X^-)$, to the neutral ground ($1^1\Sigma_g^+$) and first excited, $1^3\Sigma_u^+(a)$ states, while the band at 2.32 eV is assigned to the higher $1^3\Pi_u(b)$ and $1^1\Sigma_u^+(A)$ states; the latter two states are accidentally degenerate in the anion geometry as schematically shown in Figure 3. In our calculations, the VDEs of the transitions to the $1^1\Sigma_g^+$, $1^3\Sigma_u^+$, $1^3\Pi_u$, and $1^1\Sigma_u^+$ states of Na_2 (shown in Table 1) are 0.53, 1.22, 2.11, and 2.13 eV, respectively, which are almost the same as those by Bonacic-Koutecky and co-workers. Both calculations reproduce the VDEs for the first two bands with a reasonable accuracy, while they underestimate slightly those of the higher excited states such as the $1^3\Pi_u$ and $1^1\Sigma_u^+$ states correlated to the $Na(3^2S) + Na(3^2P)$ asymptote. Our calculations also predict the VDEs to the higher excited states ($1^3\Sigma_g^+$, $2^1\Sigma_g^+$, and $1^1\Pi_u$) in the EBE range of 2.5−3.0 eV, but no band is observed in this energy region in PES, probably because of much lower electron collection efficiency at near the energy range close to the detachment energy.

For the 1:1 complex, $Na_2^-(NH_3)$, PES exhibits five bands at 0.41, 1.36, 1.86, 2.11, and 2.40 eV as shown in Figure 1b. PES of the complex in the energy below 1.5 eV is rather similar to that of Na_2^-, while the spectrum above 1.5 eV is significantly altered by solvation. The transition to the neutral ground state

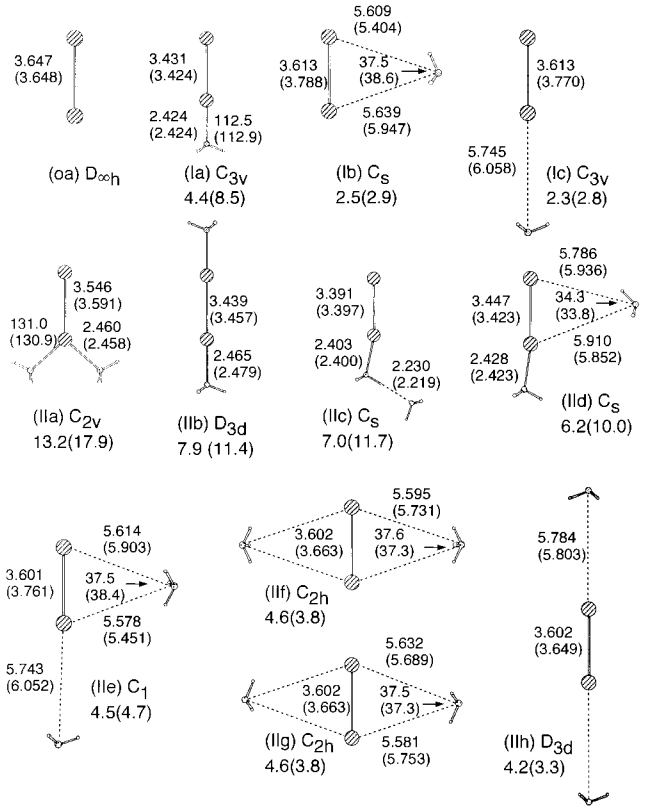

Figure 2. Optimized geometries and total binding energies of $Na_2^-(NH_3)_n$ ($n \leq 2$) at CASSCF(3E/10+3n MO)/6-31++G(d,p) level. Geometrical parameters are given in angstroms and degrees. Values in parentheses are by ROHF/6-31++G(d,p) method.

is shifted by 0.14 to the lower EBE upon complex formation, which indicates that the binding energy between the neutral Na_2 and ammonia molecule is larger than that in the anion form.

We have obtained three isomers for $Na_2^-(NH_3)$ by the calculation as shown in Figure 2. The isomer Ia has a C_{3v} structure where an ammonia molecule is bound linearly to one Na atom by the N atom. On the other hand, an NH_3 molecule is bound to Na_2^- from hydrogen side in Ib and Ic: N and two Na atoms form a triangle in Ib, while they are linear in Ic. These two isomers are almost isoenergetic and higher in energy than the Ia by ∼2 kcal/mol at CASSCF level. The VDEs of the lowest-energy band derived from the $1^1\Sigma_g^+ - 1^2\Sigma_u^+$ transition of Na_2^- are calculated to be 0.21 for Ia and ∼0.6 eV for Ib and Ic, respectively. The VDE is shifted to the red from the bare Na_2^- in the Ia and to the blue in the Ib and Ic by an addition of NH_3. Thus, the observed first band for $Na_2^-(NH_3)$ is considered to stem from the isomer with Na−N bond based on the energy relation between isomers as well as the red shift from $n = 0$ to $n = 1$, though the calculation underestimates the VDE. In addition, the observed energy difference between the two lowest bands (0.95 eV) is better reproduced by Ia (0.98 eV) than the other two (∼0.7 eV). Therefore, the first two bands can be safely assigned to the $1^1A_1 - 1^2A_1$ and $1^3A_1 - 1^2A_1$ transitions of the N-bonded cluster derived from the $1^1\Sigma_g^+ - 1^2\Sigma_u^+$ and $1^3\Sigma_u^+ - 1^2\Sigma_u^+$ transitions of the bare dimer as schematically shown in Figure 3. It is worth noticing that Na−Na distance in Ia is shortened from Na_2^- by the ligation of an NH_3, which is considered to result from the spreading of the unpaired electron in the antibonding $4\sigma_u$ orbital. These results resemble those found for $Na^-(NH_3)$; the isomer with an Na−N bond has been found to be more stable than that with Na−H bonds and their transitions to the neutral ground state are shifted to the red and to the blue with respect to that of Na^- for the former and latter

TABLE 1: Vertical Detachment Energies (VDEs) (eV) of $Na_2^-(NH_3)_n$ ($n = 0$ and 1) by the SDCI Method

$n = 0$			$n = 1$						
0a[a]			Ia[a]			Ib[a]		Ic[a]	
exp[b]	state	calc[b]	exp[b]	state	calc[b]	state	calc[b]	state	calc[b]
0.55(0.00)	$1\,^1\Sigma_g^+$	0.53(0.00)	0.41(0.00)	$1\,^1A_1$	0.21(0.00)	$1\,^1A'$	0.62(0.00)	$1\,^1A_1$	0.61(0.00)
1.38(0.83)	$1\,^3\Sigma_u^+$	1.22(0.69)	1.36(0.95)	$1\,^3A_1$	1.19(0.98)	$1\,^3A'$	1.33(0.71)	$1\,^3A_1$	1.31(0.70)
	$1\,^3\Pi_u$	2.11(1.58)	1.86(1.45)	$1\,^3E$	1.58(1.37)	$1\,^3A''$	2.19(1.57)	$1\,^3E$	2.20(1.59)
						$2\,^3A'$	2.20(1.58)		
2.32(1.77)	$1\,^1\Sigma_u^+$	2.13(1.60)	2.11(1.70)	$2\,^1A_1$	1.90(1.69)	$2\,^1A'$	2.24(1.62)	$2\,^1A_1$	2.21(1.60)
	$1\,^3\Sigma_g^+$	2.55(2.02)	2.40(1.99)	$2\,^3A_1$	2.16(1.96)	$3\,^3A'$	2.67(2.05)	$2\,^3A_1$	2.65(2.04)
	$2\,^1\Sigma_g^+$	2.88(2.35)		$3\,^1A_1$	2.52(2.31)	$3\,^1A'$	3.00(2.39)	$3\,^1A_1$	2.96(2.38)
	$1\,^1\Pi_u$	2.95(2.42)		$1\,^1E$	2.38(2.14)	$1\,^1A''$	3.04(2.43)	$1\,^1E$	3.06(2.45)
						$4\,^1A'$	3.06(2.45)		

[a] Corresponds to structures in Figure 2. [b] Values in parentheses are energy difference from neutral ground state.

TABLE 2: Vertical Detachment Energies (eV) of $Na_2^-(NH_3)_2$ Calculated by the SDCI Method

	IIa[a]		IIb[a]		IIc[a]		IId[a]		IIe[a]		IIf[a]		IIg[a]		IIh[a]	
exp[b]	state	calc[b]	state	calc[b]	state	calc[b]	state	calc[b]	state	calc[b]	state	calc[b]	state	calc[b]	state	calc[b]
0.47(0.00)	$1\,^1A_1$	0.25(0.00)	$1\,^1A_{1g}$	0.03(0.00)	$1\,^1A'$	0.08(0.00)	$1\,^1A'$	0.27(0.00)	$1\,^1A$	0.70(0.00)	$1\,^1A_g$	0.70(0.00)	$1\,^1A_g$	0.70(0.00)	$1\,^1A_{1g}$	0.70(0.00)
1.39(0.92)	$1\,^3A_1$	1.24(0.99)	$1\,^3A_{2u}$	1.17(1.14)	$1\,^3A'$	1.11(1.03)	$1\,^3A'$	1.25(0.98)	$1\,^3A$	1.41(0.71)	$1\,^3A_u$	1.44(0.74)	$1\,^3B_u$	1.44(0.74)	$1\,^3A_{2u}$	1.40(0.70)
	$1\,^3B_2$	1.46(1.21)	$1\,^3E_u$	1.14(1.11)	$1\,^3A''$	1.44(1.36)	$1\,^3A''$	1.64(1.37)	$2\,^3A$	2.29(1.59)	$1\,^3B_u$	2.29(1.59)	$1\,^3A_u$	2.29(1.59)	$1\,^3E_u$	2.30(1.60)
	$1\,^3B_1$	1.51(1.26)			$2\,^3A'$	1.44(1.36)	$2\,^3A'$	1.64(1.37)	$3\,^3A$	2.29(1.59)	$2\,^3B_u$	2.29(1.59)	$2\,^3B_u$	2.29(1.59)		
1.90(1.43)	$2\,^1A_1$	1.77(1.52)	$1\,^1A_{2u}$	1.53(1.50)	$2\,^1A'$	1.84(1.76)	$2\,^1A'$	1.98(1.71)	$2\,^1A$	2.32(1.62)	$1\,^1A_u$	2.35(1.65)	$1\,^1B_u$	2.35(1.65)	$1\,^1A_{2u}$	2.30(1.60)
2.17(1.70)	$2\,^3A_1$	1.88(1.63)	$1\,^3A_{1g}$	1.63(1.60)	$3\,^3A'$	2.09(2.01)	$3\,^3A'$	2.26(1.99)	$4\,^3A$	2.76(2.06)	$1\,^3A_g$	2.79(2.09)	$1\,^3A_g$	2.79(2.09)	$1\,^3A_{1g}$	2.74(2.04)
	$3\,^1A_1$	2.31(2.06)	$2\,^1A_{1g}$	1.93(1.90)	$4\,^1A'$	2.42(2.34)	$4\,^1A'$	2.62(2.35)	$3\,^1A$	3.09(2.39)	$2\,^1A_g$	3.12(2.42)	$2\,^1A_g$	3.12(2.42)	$3\,^1A_{1g}$	3.06(2.36)
	$1\,^1B_2$	2.11(1.86)	$1\,^1E_u$	1.86(1.83)	$3\,^1A''$	2.23(2.15)	$1\,^1A''$	2.45(2.18)	$4\,^1A$	3.14(2.44)	$1\,^1B_u$	3.14(2.44)	$1\,^1A_u$	3.14(2.44)	$1\,^1E_u$	3.15(2.45)
	$1\,^1B_1$	2.13(1.88)			$1\,^1A'$	2.23(2.15)	$3\,^1A'$	2.46(2.19)	$5\,^1A$	3.15(2.45)	$2\,^1B_u$	3.17(2.47)	$2\,^1B_u$	3.17(2.47)		

[a] Corresponds to structures in Figure 2. [b] Values in parentheses are energy difference from neutral ground state.

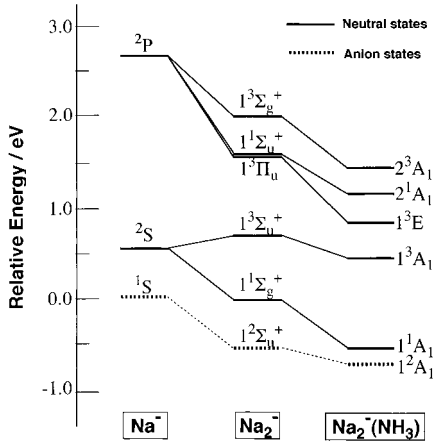

Figure 3. Schematic energy level diagrams for Na^-, Na_2^-, and $Na_2^-(NH_3)$ and those for their neutral states based on the theoretical calculations. For $Na_2^-(NH_3)$, the results on the most stable isomer (Ia in Figure 2 and Table 1) are plotted.

isomers, respectively. The diffusification of SOMO has also been found to occur in $Na(NH_3)_n$ with increasing n.[22]

On the other hand, the bands at 1.86 and 2.11 eV may be ascribed to the $1^3E-1^2A_1$ and $2^1A_1-1^2A_1$ transitions derived from the degenerate $1^3\Pi_u-1^2\Sigma_u^+$ and $1^1\Sigma_u^+-1^2\Sigma_u^+$ transitions of Na_2^- as follows (see also Figure 3). In the most stable C_{3v} geometry of $Na_2^-(NH_3)$, the $2\pi_u$ orbitals of Na_2 may be more stabilized than $4\sigma_u$ by mixing with the σ^* orbitals of N−H due to the smaller separation in orbital energy. In addition, the mixing of the lone-pair orbital of NH_3 is considered to destabilize the $4\sigma_u$ orbital. As a result, the 1^3E state derived from the $1^3\Pi_u$ state of Na_2 is expected to become lower than the 2^1A state originating from the $1^1\Sigma_u^+$ state in the complex. The calculations support this expectation having the 1^3E state below the 2^1A_1 states by 0.32 eV (see Table 1). Thus, we assign the shoulder at 1.86 eV and the peak at 2.11 eV to the transitions to the 1^3E and 2^1A_1 states in Ia, respectively. As for the relatively strong band observed at 2.40 eV, our calculations also predict that the VDEs to the 2^3A_1 and 1^1E states are below 2.50 eV. Since the present calculations tend to underestimate the VDEs for the higher excited states correlating to the $Na(3^2S) + Na(3^2P)$ asymptote, we tentatively assign the 2.40 eV band to the transition to the 2^3A state derived from $Na_2(^3\Sigma_g^+)$. We also observe weak humps in the energy region below and above 3.0 eV as shown in Figure 1b. At present, we cannot assign these transitions definitively.

As shown in Figure 1b, the PES band of the neutral ground state of $Na_2(NH_3)$ has much wider bandwidth than the sodium dimer itself. The broad-band feature may indicate the contribution of the second isomer with the Na−H bonds to the spectral intensity in this energy region. In fact, these isomers are calculated to be less stable by only ∼2 kcal/mol and their VDEs to the neutral ground state are estimated to be 0.61−0.62 eV as shown in Table 1. To characterize the less stable isomer further, the PES experiment with higher resolution is now in progress.

PES of $Na_2^-(NH_3)_2$ (Figure 1c) shows four distinct bands at 0.47, 1.39, 1.90, and 2.17 eV. With the addition of the second ammonia molecule, the EBE of the two lowest bands increases by ca. 0.06 and 0.03 eV, respectively, with respect to those of the 1:1 complex. We obtain eight minimum structures (IIa−h in Figure 2) by the calculation. The most stable isomer has a C_{2v} geometry (IIa), in which two ammonia molecules are bound to one of the Na atoms by their N atoms. The structure IIb, in which each NH_3 molecule is bound to different Na atoms, is the second most stable, while the IIc that the second NH_3 binds the Ia through hydrogen bond is almost isoenergetic to the IIb. These two isomers are higher in energy than IIa by ∼5 kcal/mol. On the other hand, the structures IId−h, where one or both NH_3 molecules are bound to Na_2^- from hydrogen sides, are less stable than IIa by more than 7 kcal/mol. Therefore, the structure where one of Na atoms is selectively ammoniated from N side is the most probable candidate for $n = 2$ cluster. The calculated VDEs are also helpful to discuss the relation between

the cluster geometry and PES bands. As seen in Table 2, VDEs of the transitions to the neutral ground state for IIe−h are shifted to higher EBE by solvation. This change is opposite to the experimental result and therefore structures having all NH_3 molecule bind by Na−H interaction are considered not to be responsible for the observed PES bands. The structures IIb and IIc should be also ruled out because their VDEs to the neutral ground state further decrease from 1:1 complex which is inconsistent with the experiment. On the other hand, the calculated VDEs to the two lowest states of IId are close to those of the most stable IIa, while the VDEs to the higher excited states are larger in IId than in IIa. Taking into account the fact that our calculations tend to underestimate the VDEs to the high-lying states, all observed bands can be regarded as those of IIa rather than IId. We can assign the 0.47 and 1.39 eV bands to the transitions to the $^1A_1$ and $^3A_1$ states in IIa derived from the $1^1\Sigma_g^+ - 1\ ^2\Sigma_u^+$ and $1^3\Sigma_u^+ - 1\ ^2\Sigma_u^+$ transitions of Na_2^-, while two distinct bands at 1.90 and 2.17 eV are ascribed to the transitions to the 2^1A_1 and 2^3A_1 states derived from the $1^1\Sigma_u^+ - 1^2\Sigma_u^+$ and $1^3\Sigma_g^+ - 1^2\Sigma_u^+$ transitions of the bare dimer anion, respectively. The amount of red-shifting of these higher-energy bands is more than 0.2 eV with respect to those of $Na_2^-(NH_3)$ and is consistent with the calculated numbers as shown in Tables 1 and 2. Although the 1^3E-type band is observed at 1.86 eV for $n = 1$ as seen in Figure 1b, this transition cannot be identified definitively for $n = 2$ and seems to be superimposed on the strong $1^3\Sigma_u^+$-type band at 1.39 eV as a result of its large red-shifting.

For $n = 3$, we have optimized three possible structures and compared their binding energies at ROHF level, since the Na−N interaction is much stronger than the Na−H and hydrogen-bond interactions for $n \leq 2$. One is a C_3 structure in which all NH_3 molecules are bound to one of the Na atoms from N side. Its optimized Na−Na and Na−N lengths are 3.876 and 2.468 Å, respectively, and Na−Na−N angle is 114.0°. Another is a C_s isomer where the third NH_3 is bound to the "free" Na in IIa by N atom, and the last one has a C_s structure where an NH_3 molecule is bound to IIa through hydrogen bond as a second-shell ligand. The calculated total binding energy of the C_3 isomer is 26.5 kcal/mol, which is larger than those of the other two by more than ∼5 kcal/mol. Therefore, the PES band for $Na_2^-(NH_3)_3$ can be ascribed to the isomer that has the maximum number of NH_3 bound to a single Na atom by Na−N bonds, and spectral change by a stepwise solvation for $n \leq 2$ is expected to continue to $n = 3$. The observed spectra shown in Figure 1d is consistent with these theoretical results. The positions of two lowest-energy bands are almost unchanged from $n = 2$, while the higher bands keep red-shifting. Though we have not carried out the CI calculation to estimate the VDEs due to the computational expense, the observed bands are probably assignable to the $1^1\Sigma_g^+$-, $1^3\Sigma_u^+$-, $1^1\Sigma_u^+$-, and $1^3\Sigma_g^+$-type transitions of the cluster in which one Na atom is selectively solvated by NH_3 molecules forming three Na−N bonds.

For larger clusters, the photoelectron bands for the higher excited states keep red-shifting, while the $1^3\Sigma_u^+$-type state starts to shift to the higher EBE for $n \geq 4$. As a result, the transitions to the higher excited states are almost superimposed on the $1^3\Sigma_u^+$-type band as seen in Figure 1, e and f.

In Figure 4, VDEs for the $1^1\Sigma_g^+$-, $1^3\Sigma_u^+$-, $1^3\Pi_u$-, $1^1\Sigma_u^+$-, and $1^3\Sigma_g^+$-type states are plotted as a function of $(n + 1.2)^{-1/3}$.[36] As the number of ammonia molecules increases, VDEs to the $1^1\Sigma_u^+$- and $1^3\Sigma_g^+$-type states decrease monotonically with similar energy separation. These states are correlated to the Na(^{2}S) + Na(^{2}P) asymptote in the bare Na_2. Thus, the extensive

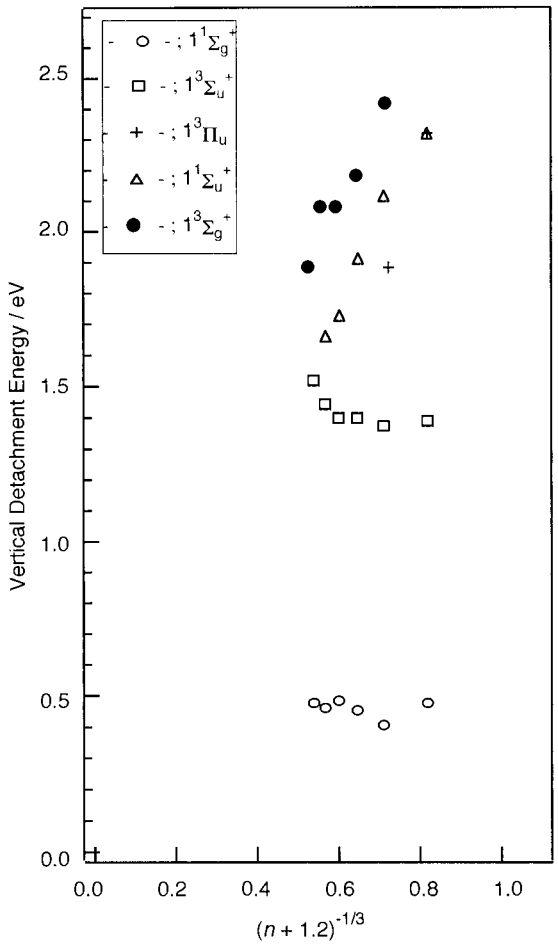

Figure 4. Vertical detachment energies of the observed transitions for $Na_2^-(NH_3)_n$ ($n \leq 5$) plotted as a function of $(n + 1.2)^{-1/3}$.

red-shifting of these transitions is coincident with the rapid decrease observed in the VDE to the Na(^{2}P)-type state for Na-$(NH_3)_n$ ($n \leq 4$). In the latter clusters, this change has been ascribed to the delocalization of unpaired electron as well as the large destabilization of 3s orbital by the strong Na−N interaction. As mentioned previously, both experimental and theoretical results indicate that ammonia molecules in $Na_2^-(NH_3)_n$ ($n \leq 3$) are bound selectively to one of the Na atoms by N atoms. Therefore, these results suggest that the similar delocalization of 3s valence electron on the ammoniated Na atom in Na_2 occurs as in the case of $Na(NH_3)_n$, and as a result, the Na−N bond becomes to some extent ionic. The slight red-shifting of the transition to the neutral ground state, indicating the larger solvation energy of the neutral form than that of anion, strongly supports this conclusion.

Figure 4 also displays that the $1^3\Sigma_u^+$-type transition starts to be shifted to higher EBE for $n \geq 4$, though the energy separation between this state and the neutral ground state is almost constant for $n = 3$. These changes seem to be related to the solvation structure of $Na_2^-(NH_3)_n$. The first solvation shell of Na atom in $Na(NH_3)_n$ has been known to complete with four or five NH_3 molecules,[20] and thus the bonding of the ligated Na atom in $Na_2^-(NH_3)_n$ is considered to be saturated with three NH_3 molecules and a counterpart Na atom. Then further ammonia molecules may form the second shell or may be directly bound to the second Na atom. In the former case, the second-shell ammonia molecules are bound to those in the first shell with a weak hydrogen bond and the spectral change of $Na_2^-(NH_3)_n$ ($n \geq 4$) is expected to be much smaller as in the case of $Na(NH_3)_n$ ($n \geq 4$). The observed rapid red-shifting of the $1^1\Sigma_u^+$- and $1^3\Sigma_g^+$-

type transitions as well as the sudden commencement of the blue shift for the $1^3\Sigma_u^+$-type transition at $n = 4$ may suggest the ligation of additional ammonia molecules to the second Na atom in the Na_2 core. However, further study is necessary to analyze why only the transition to the $1^3\Sigma_u^+$-type state is blue-shifted.

In conclusion, we have investigated the ammoniated Na dimer anions with the photoelectron spectroscopy and the ab initio MO method. Na dimer is found to be asymmetrically solvated; ammonia molecules are bound selectively to one of the Na atoms in the clusters with n up to 3. As in the case of $Na^-(NH_3)_n$ reported in the previous paper, the spectra of $Na_2^-(NH_3)_n$ ($n \leq 3$) exhibit the large red shifts of the transitions to the higher excited states correlated to the $Na(^2S) + Na(^2P)$ asymptote as well as the slight red shift of the neutral ground state. These spectral changes are ascribed to the delocalization of 3s valence electron on the ammoniated Na atom in Na_2 and the formation of ion pair state being similar to that of $Na^-(NH_3)_n$. We have also found that the additional ammonia molecules in $n \geq 4$ may be bound to the second Na atom of Na_2 and induce further interesting spectral changes. This study is the first attempt to explore the solvation process of metal aggregate in small polar solvent clusters. Extension of these experimental and theoretical investigation to higher cluster size for both the metal atom and solvent molecules is now in progress.

Acknowledgment. This work was partially supported by Grants-in-Aid from the Ministry of Education, Science, Sports and Culture of Japan. We are also grateful to the Aichi Science and Technology Foundation and Japan Society for the Promotion of Science for financial support. All computations were carried out at the Computer Centers at Tokyo Metropolitan University and at Institute for Molecular Science.

References and Notes

(1) Dogonadze, R. R., Kalman, E., Kornyshev, A. A., Ulstrup, J. Eds. *The Chemical Physics of Solvation*; Elsevier: Amsterdam 1988; Part C.
(2) Tuttle, Jr., T. R.; Golden, S. J. *Phys. Chem.* **1991**, *95*, 5725.
(3) Alfano, J. C.; Walhout, P. K.; Kimura, Y.; Barbara, P. F. *J. Chem. Phys.* **1993**, *98*, 5996.
(4) H. Haberland, H.; Schindler, H.-G. Worksnop, D. R. *Ber. Bunsen-Ges. Phys. Chem.* **1984**, *88*, 270.
(5) Haberland, H.; Ludewigt, C.; Schindler, H.-G.; Worksnop, D. R. *Surf. Sci.* **1985**, *156*, 157.
(6) Coe, J. V.; Lee, G. H.; Eaton, J. G.; Sarkas, H. W.; Bowen, K. H.; Ludewigt, C.; Haberland, H.; Worsnop, D. R. *J. Chem. Phys.* **1990**, *92*, 3980.
(7) Lee, G. H.; Arnold, S. T.; Eaton, J. G.; Sarkas, H. W.; Bowen, K. H.; Ludewigt, C.; Haberland, H. *Z. Phys.* **1991**, *D20*, 9.
(8) Barnett, R. N.; Landman, U.; Cleveland, C. L.; Jortner, J. *Chem. Phys. Lett.* **1988**, *145*, 382.
(9) Barnett, R. N.; Landman, U.; Cleveland, C. L.; Kestner, N. R.; Jortner, J. *Chem. Phys. Lett.* **1988**, *148*, 249.
(10) Ayotte, P.; Johnson, M. A. *J. Chem. Phys.* **1997**, *106*, 811.
(11) Hertel, I. V.; Hüglin, C.; Nitsch, C.; Schulz, C. P. *Phys. Rev. Lett.* **1991**, *67*, 1767.
(12) Misaizu, F.; Tsukamoto, K.; Sanekata, M.; Fuke, K. *Chem. Phys. Lett.* **1992**, *188*, 241.
(13) Takasu, R.; Hashimoto, K.; Fuke, K. *Chem. Phys. Lett.* **1996**, *258*, 94.
(14) Takasu, R.; Misaizu, F.; Hashimoto, K.; Fuke, K. *J. Phys. Chem.* **1997**, *A101*, 3078.
(15) Martyna, G. J.; Klein, M. L. *J. Phys. Chem.* **1991**, *95*, 515.
(16) Barnett, R. N.; Landman, U. *Phys. Rev. Lett.* **1993**, *70*, 1775.
(17) Stampfli, P.; Bennemann, K. H. *Comput. Mater. Sci.* **1994**, *2*, 578.
(18) Hashimoto, K.; He, S.; Morokuma, K. *Chem. Phys. Lett.* **1993**, *206*, 297.
(19) Hashimoto, K.; Morokuma, K. *J. Am. Chem. Soc.* **1994**, *116*, 11436.
(20) Hashimoto, K.; Morokuma, K. *J. Am. Chem. Soc.* **1995**, *117*, 4151.
(21) Hashimoto, K; Kamimoto, T. *J. Am. Chem. Soc.* **1998**, *120*, 3560.
(22) Hashimoto, K.; Kamimoto, T.; Fuke, K. *Chem. Phys. Lett.* **1997**, 266, 7.
(23) Takasu, R.; Taguchi, T.; Hashimoto, K.; Fuke, K. *Chem. Phys. Lett.* **1998**, 290 481.
(24) Brockhaus, P.; Hertel, I. V.; Schulz, C. P. *J. Chem. Phys.*, in press.
(25) Misaizu, F.; Tsukamoto, K.; Sanekata, M.; Fuke, K. *Laser Chem.* **1995**, *15*, 195.
(26) Werner, H.-J.; Knowles, P. J.,*J. Chem. Phys.* **1985**, *82*, 5053.
(27) Knowles, P. J.; Werner, H.-J. *Chem. Phys. Lett.* **1985**, *115*, 259.
(28) Werner, H.-J.; Knowles, P. J. *J. Chem. Phys.* **1988**,*89*, 5803.
(29) Knowles, P. J.; Werner, H.-J. *Chem. Phys. Lett.* **1988**, *145*, 514.
(30) Knowles, P. J.; Werner, H.-J. *Theor. Chim. Acta* **1992**, *84*, 95.
(31) Schmidt, M. W.; Baldridge, K. K.; Boatz, J. A.; Elbert S. T.; Gordon, M. S.; Jensen, J. H.; Koseki S.; Matsunaga N.; Nguyen, K. A.; Su, S. J.; Windus, T. L.; Dupuis, M.; Montogomery, J. A. *J. Comput. Chem.* **1993**, *14*, 1347.
(32) MOLPRO is a package of ab initio programs written by H.-J. Werner and P. J. Knowles, with contributions of J. Almlof, R. D. Amos, M. J. O. Deegan, S. T. Elbert, C. Hampel, W. Meyer, K. Peterson, R. Pitzer, A. J. Stone, P. R. Taylor, R. Lindh, M. E. Mura, and T. Thorsteinsson.
(33) McHugh, K. M.; Eaton, J. G.; Lee, G. H.; Sarkas, H. W.; Kidder, L. H.; Snodgrass, J. T.; Manaa, M. R.; Bowen, K. H. *J. Chem. Phys.* **1989**, *91*, 3792.
(34) Bonacic-Koutecky, V.; Fantucci, P.; Koutecky, J. *J. Chem. Phys.* **1989**, *91*, 3794.
(35) Bonacic-Koutecky, V.; Fantucci, P.; Koutecky, J. *J. Chem. Phys.* **1990**, *93*, 3802.
(36) The VDEs of five transitions are plotted by assuming a classical droplet model described in ref 37. The radius of a cluster containing n ammonia molecules is calculated by approximating the molecular volumes of Na_2 and ammonia as those being estimated from their densities (the volume of Na_2 is assumed to be two times of that of Na).
(37) Markovich, G.; Pollack, S.; Giniger, R.; Cheshnovsky, O. *J. Chem. Phys.* **1994**, *101*, 9344.